




In Vitro Intestinal Uptake And Permeability Of Fluorescently-Labelled Hyaluronic Acid Nanogels

This article was published in the following Dove Press journal:
International Journal of Nanomedicine

Miguel Xavier ¹
Lorena García-Hevia ¹
Isabel R Amado^{1,2}
Lorenzo Pastrana¹
Catarina Gonçalves ¹

¹Department of Life Sciences,
International Iberian Nanotechnology
Laboratory, Braga 4715-330, Portugal;

²Department of Food and Analytical
Chemistry, Faculty of Sciences, University
of Vigo, Ourense 32004, Spain

Background: Oral administration remains the most common mode of drug delivery. However, orally administered bioactive compounds must first survive digestion and then be absorbed at the intestine in order to reach other tissues or organs. The efficiency of both processes can be improved by encapsulation or conjugation with polymeric nanoparticles. Here we report the synthesis of amphiphilic hyaluronic acid (HyA) nanogels as nanocarriers for drug delivery.

Methods: HyA nanogels were prepared by self-assembly from amphiphilic HyA conjugates produced by grafting hydrophobic alkyl chains to the HyA backbone. The dye Cy5.5 was covalently bonded and used for tracking. The nanogels were characterised according to their structure, size and zeta potential, as well as biocompatibility towards an intestinal epithelial cell line. The uptake and intestinal permeability of the nanogels were assessed using in vitro models, which physiological relevance was verified regarding the morphology of the epithelium, the production of mucus, the expression of occludin and the transepithelial electrical resistance.

Results: The covalent binding of Cy5.5 did not affect significantly the size and surface charge of the nanogels at 125.1 ± 3.2 nm and -57.6 ± 6.2 mV respectively after labelling. Studies of biocompatibility showed that the nanogels were non-toxic to Caco-2 cells up to the concentration of $0.1 \text{ mg}\cdot\text{mL}^{-1}$. The presence of mucus affected the nanogel uptake and highlighted the importance of considering mucus-producing cells in in vitro intestinal models. The uptake or adsorption to a Caco-2/HT29-MTX co-culture (8.1%) was higher than with single Caco-2 cell cultures (4.3%). Interestingly, both models led to minute (<0.5%) permeation of the nanogels across the intestinal barrier.

Conclusion: The HyA nanogels demonstrated to be mucoadhesive and effectively uptaken by intestinal cells. Both are determinant features for sustained release, but if systemic delivery is envisaged further modification with targeting moieties could be important to improve the nanogel permeability.

Keywords: oral delivery, in vitro models, nanogels, intestinal permeability, cellular uptake

Introduction

Oral administration remains the preferred route for drug delivery owing to its low invasiveness, high efficiency and increased patient compliance.¹ However, digestion through the gastro-intestinal tract and absorption in the small intestine constitute two obstacles that limit respectively the bioaccessibility and bioavailability of orally administered compounds.² Thus, the development of smart carrier materials that are capable of resisting digestion and deliver their cargo through the intestinal epithelium is key to the success of newly developed drugs or food supplements. Equally important is the reliability of in vitro models to predict

Correspondence: Catarina Gonçalves
Department of Life Sciences, International
Iberian Nanotechnology Laboratory, Av.
Mestre José Veiga s/n, Braga 4715-330,
Portugal
Email catarina.goncalves@inl.int

absorption at the intestine. These models not only allow the reduction of the use of animal models in *in vivo* studies, in line with the 3Rs principles of replacement, reduction and refinement, but also allow the use of human cells, thus reducing interspecies variability and potentially increasing the likelihood of new drugs to reach the market.^{1,3}

In vitro models of the intestinal epithelium have existed for around 30 years.⁴ The gastro-intestinal epithelium consists of a layer of epithelial cells, which include but are not limited to, enterocytes, goblet cells, intraepithelial lymphocytes and dendritic cells.^{5,6} From these, the most abundant are enterocytes, which main function is the absorption of nutrients. Caco-2 are human colorectal adenocarcinoma epithelial cells. When reaching confluency, Caco-2 differentiate spontaneously to form a cell monolayer with an apical brush border and properties typical of absorptive enterocytes found in the small intestine.⁷ Cultivation of Caco-2 cells on filter supports further improves their morphological and functional differentiation and Caco-2 have been found to form a polarised epithelium with characteristic microvilli, closely sealed by tight junctions (TJs) and which expresses typical metabolic enzymes and membrane uptake/efflux transporters.^{1,2,7-9} Interestingly, Caco-2 monolayers are less permeable via the paracellular pathway when compared to the *in vivo* epithelium.^{2,10,11} Caco-2 cells also do not produce mucus, resulting in an enhanced transport of small molecules which diffuse more easily in the absence a mucous barrier. To better approximate the physiology of the intestinal mucosa, co-culture of Caco-2 cells with additional cell types, such as goblet cells, has become common practice in academia.¹²⁻¹⁶

Polymeric nanogels have been the target of extensive research as nanocarriers for bioactive compounds, offering prolonged blood circulation times and enhancing drug solubility.¹⁷⁻¹⁹ Hyaluronic acid (HyA) is a natural, hydrophilic glycosaminoglycan, which has been used for its biocompatibility, mucoadhesive properties, specificity to certain cellular receptors and, the presence of reactive groups that allow for functional chemical modifications.¹⁷⁻²³ The conjugation of biopolymers with fluorescent probes is useful for tracking in both *in vitro* and *in vivo* biological studies. However, the incorporation of dyes in nanostructures must be stable in order to prevent leakage, which could lead to misinterpretation in studies on biodistribution or cellular uptake.²⁴ In addition, the use of fluorophores may also alter relevant properties of the nanogels, such as their size or

surface charge, potentially affecting their capacity to work as nanocarriers.²⁵

In this work, the synthesis of fluorescently-labelled HyA nanogels for oral delivery of bioactive compounds is reported. The nanogels were prepared by self-assembly from amphiphilic HyA conjugates produced by grafting hydrophobic alkyl chains to the HyA backbone. The dye Cy5.5 was used as a reporter to quantify the cellular uptake of the nanogels and their permeation through the intestinal epithelium. The nanogels were characterised according to their structure, size and zeta potential, as well as biocompatibility towards an intestinal epithelial cell line. The uptake and permeation of the nanogels were tested using cell-based *in vitro* models, which included Caco-2, HT-29, HT29-MTX and co-culture combinations thereof to mimic the intestinal epithelium. The 5 culture conditions were characterised in terms of the topography of the cell layers, the expression of tight junction proteins and the integrity of the epithelial barrier. In addition, HT29-MTX, as mucin-secreting mature goblet cells,^{12,16,26,27} also allowed to study the mucoadhesion of the HyA nanogels.

Materials And Methods

Materials

Low molecular weight (4.8 kDa) hyaluronic acid (HyA) was purchased from Lifecore Biomedical (Chaska, MN, USA). Cy[®]5.5 hydrazide was obtained from GE Healthcare (Chicago, IL, USA). AG 50W-X8 resin was obtained from Bio-Rad (Hercules, CA, USA). Methanol was obtained from Honeywell Riedel-de-Haën[™] (Seezel, Germany) and acetic acid from Fisher Scientific (Hampton, NH, USA). Minimum essential media (MEM) and 4', 6-diamidino-2-phenylindole, dilactate (DAPI, Invitrogen[™]) were purchased from Thermo Fisher Scientific (Waltham, MA, USA). 8-well chamber μ -slides were acquired from Ibidi GmbH (Gräfelfing, Germany). Trypsin-EDTA (0.25% trypsin; 0.1% EDTA), penicillin/streptomycin 100x, foetal bovine serum (FBS), Hank's balanced salt solution (HBSS), non-essential amino acids (NEAA), 1- μ m pore size transwell[®] inserts and Amicon[®] Ultra-15 centrifugal filters were bought from Merck Millipore (Burlington, MA, USA). Chloroform, N-(3-Dimethylaminopropyl)-N'-ethylcarbodiimide (EDC), N-hydroxysuccinimide (NHS), Triethylamine (TEA), tetrabutylammonium fluoride (TBA-F), deuterium oxide (D₂O), hexadecylamine (C16), sodium chloride (NaCl), dimethyl sulfoxide (DMSO), paraformaldehyde (PFA), 1% alcian blue solution in 3% acetic acid (alcian blue 8XG), Triton[™]

X-100, phalloidin-tetramethylrhodamine B isothiocyanate (phalloidin-TRITC), bovine serum albumin (BSA), fluoroshield™, L-glutamine solution 200 mM, sodium pyruvate solution 100 mM, resazurin sodium salt, and Dulbecco's modified Eagle's Medium-high glucose (DMEM) were obtained from Sigma-Aldrich (St. Louis, MO, USA).

Chemical Modifications Of Hyaluronic Acid (HyA)

Synthesis Of Amphiphilic Hyaluronic Acid Conjugate (C16-HyA)

The synthesis of amphiphilic HyA conjugates was adapted from previous methods.¹⁷ Briefly, HyA sodium salt was solubilised in DMSO following Na⁺ ion exchange by tetrabutylammonium (TBA) using a cation exchange resin (Figure 1A). EDC (155 mg) and NHS (93 mg) were added to the HyA-TBA solution in DMSO (500 mg; 1% w/v) followed by the addition of a solution of C16 (58 mg) in DMSO and 51 μL of TEA (Figure 1B). The mixture reacted under stirring for 24h at 50 °C, and the resulting solution was dialysed (3.5 kDa MWCO) against 150 mM NaCl for 3 days followed by diH₂O for 2 days. The samples were dispersed in D₂O at 10 mg·mL⁻¹ and the degree of substitution (DS) of C16 molecules in the HyA was determined by ¹H NMR using a Varian Unity Plus 300 spectrometer operating at 299.94 MHz and 25 °C. The DS was obtained following Equation 1, where A and B are the integral values corresponding to the protons of the CH₃ group of the alkyl chain (δ = 0.8–1.0 ppm) and the signal from the disaccharide protons (δ = 3.51–4.61 ppm) respectively.

$$DS_{C16} = \frac{11}{3} \times \frac{A}{B} \times 100 \quad (1)$$

Cy5.5-Labeling Of C16-HyA

Cy5.5 hydrazide (1 mg·mL⁻¹ in PBS) was added to a dispersion of C16-HyA (40 mg in 14 mL PBS) at a molar ratio of 1.6% over the free carbonyl groups of the HyA (after subtracting those used in the grafting of the C16 chains). The mixture was stirred overnight at 50 °C to promote the formation of stable amide bonds from the reaction of the hydrazide esters with the HyA carbonyl groups (Figure 1C). The resulting solution was dialysed (12–14 kDa MWCO) against PBS and diH₂O, and purified using 10 kDa MWCO Amicon Ultra-15 centrifugal filters, until free Cy5.5 could not be detected in the eluate by fluorescence spectroscopy (λ_{ex}=650 nm, λ_{em}=675–800 nm) measured using a BioTeK[®] Synergy H1 (Winoski, VT, USA) multi-plate reader. The yield after filtration

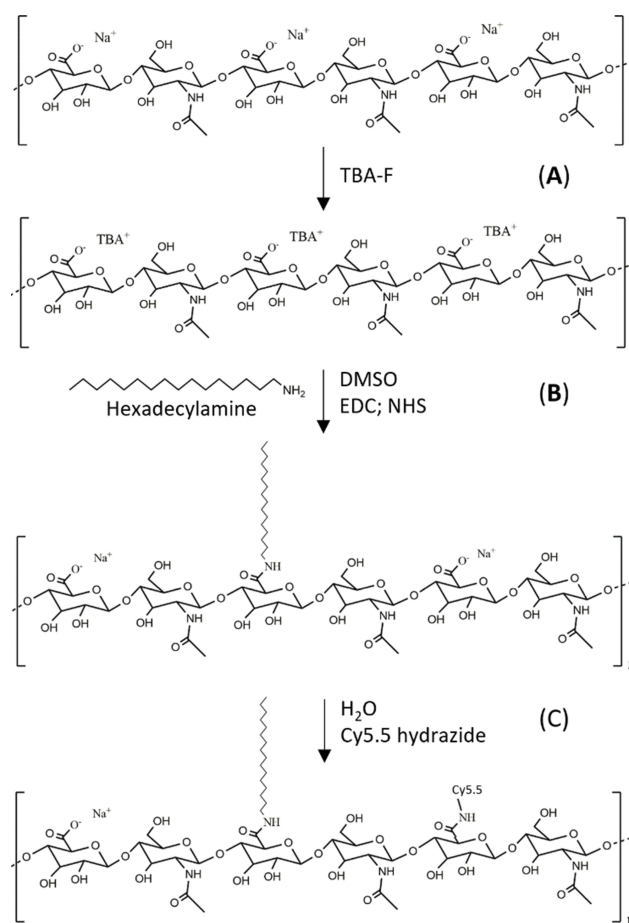


Figure 1 Schematic illustration of the methodology used for the synthesis of the C16-HyA-Cy5.5 conjugates. (A) Ion exchange using tetrabutylammonium fluoride (TBA-F) (B) Grafting of hexadecylamine (C16) to the HyA backbone using EDC/NHS (C) Grafting of Cy5.5 hydrazide fluorophore in H₂O by the formation of stable amide bonds.

through the 10 kDa Amicon filters was estimated at 87% according to the fluorescence readings. The effective DS of Cy5.5 in the C16-HyA-Cy5.5 conjugate was not quantified as this was not relevant for this study, where Cy5.5 was used just for tracking.

Synthesis And Characterisation Of HyA Nanogels

Synthesis Of HyA Nanogels

Nanogels were obtained by dispersion of C16-HyA or C16-HyA-Cy5.5 in milli-Q diH₂O at 0.5 mg·mL⁻¹ under stirring at 50 °C, followed by 2 sonication cycles (37 kHz; 104 W) for 15 min and filtration through a 0.45 μm PVDF syringe filter (Millex, Millipore). The stability of the nanogel dispersions was monitored by measuring the average size and polydispersity index (PDI) for up to 48 days.

Size And Zeta Potential

The hydrodynamic diameter (size) and surface charge (zeta potential) of the HyA nanogels were measured by dynamic light scattering (DLS) using a SZ-100 nanoparticle analyser (Horiba Scientific, Kyoto, Japan). Nanogels dispersed at 1 mg·mL⁻¹ were measured at 25 °C using a He-Ne laser (633 nm) and a detector angle of 173°. Polystyrene cells and folded capillary cells were used for size and zeta potential measurements respectively. Data are expressed as mean ± SD from 6 independent measurements.

Cell Culture

All cells were maintained in media with 100 U·mL⁻¹ penicillin and 100 µg·mL⁻¹ streptomycin (1% Pen/Strep), in a humidified chamber at 37 °C and 5% CO₂. The culture media was replenished every 2–3 days and the cells were routinely sub-cultured assuring a maximum confluence of 70–80%. To detach adherent cells, trypsin-EDTA was used for 5–10 min.

Caco-2

Caco-2 cells, clone HTB-37™, from human colon carcinoma (passages 25–40), were obtained from the American Type Culture Collection (ATCC®) and cultured in minimum essential media (MEM) supplemented with 20% FBS, 1% non-essential amino-acids (NEAA) and 1 mM sodium pyruvate.

HT-29

HT-29 cells (passages 20–25), originally obtained from the American Type Culture Collection (ATCC®), were grown in DMEM supplemented with 10% FBS and 1 mM sodium pyruvate.

HT29-MTX

Mucus-secreting HT29-MTX-E12 cells (passages 60–65), were obtained from the European collection of Authenticated Cell cultures (ECACC) and cultured in DMEM, supplemented with 2mM L-glutamine, 10% foetal calf serum (FCS) and 1% NEAA.

In Vitro Cytotoxicity Assay

The cytotoxicity of the HyA nanogels was determined indirectly by the resazurin reduction assay. Caco-2 cells were plated in 96-well plates at 3×10⁴ cells·cm⁻¹. After 24h, the media was removed and replenished with fresh media supplemented with 10 µg·mL⁻¹ resazurin sodium salt. HyA nanogels dispersed in PBS 1x were added (10% of total volume) to yield the final concentrations of 0.01, 0.05 and

0.1 mg·mL⁻¹. PBS (10% v/v) and DMSO (40% v/v) were used as negative and positive controls, respectively. The cells were incubated for 24h and 48h and the cell metabolic activity was determined by measuring the fluorescence of resofurin (λ_{ex}=560 nm, λ_{em}=590 nm). The results are expressed as a percentage in relation to the negative control.

In Vitro Intestinal Epithelium Models

To evaluate the capacity to mimic the intestinal epithelium, monocultures of Caco-2, HT-29 and HT29-MTX, as well as co-cultures of Caco-2/HT-29 and Caco-2/HT29-MTX were used. For the co-cultures, the ratio of Caco-2 over HT-29 or HT29-MTX was 9:1 and the media used was MEM supplemented with 20% FBS, 1% non-essential amino-acids (NEAA) and 1 mM sodium pyruvate. To assess the production of mucus, the expression of the tight junction protein occludin, the uptake of the HyA nanogels and, the topography and polarization of the cell layers, cells were plated in 8-well µ-slides at a seeding density of 4.4×10⁴ cells·cm⁻² and grown for 21 days. To determine the integrity of the epithelial barrier and its permeability to the HyA nanogels, Caco-2 or Caco-2/HT29-MTX co-cultures were seeded at 1×10⁵ cells·cm⁻² and grown for 21 days on the apical chamber of 1-µm pore size transwell® inserts.

Alcian Blue Staining

Cultures were washed with PBS and fixed in cold methacarn (60% methanol, 30% chloroform, 10% acetic acid) for 15 min at 4 °C to preserve the mucus layer.¹⁴ Cells were then washed in a 3% acetic acid solution in H₂O, stained with alcian blue 8XG for 15 min at RT, washed with water and imaged using an optical microscope.

Immunocytochemistry

To evaluate the topography and polarization of the cells and the expression of the tight junction protein occludin, cells were fixed in 4% (w/v) paraformaldehyde for 20 min and permeabilised by incubation with a 0.2% (v/v) Triton X-100 solution in PBS for 10 min. The fixed cultures were then incubated in a 2% (w/v) BSA solution in PBS to minimise non-specific antibody bonding. After blocking, cells were incubated with 5 µg·mL⁻¹ Alexa Fluor® 488-conjugated occludin monoclonal antibody (OC-3F10) for 1h followed by incubation with phalloidin-TRITC for 1h. Finally, cells were washed extensively, counter-stained with DAPI (0.2 µg·mL⁻¹) for 10 min and preserved in Fluoroshield mounting medium. The stained cell layers

were imaged using a Zeiss LSM780 confocal laser scanning microscope (Oberkochen, Germany) and analysed using Zen 2010 software and ImageJ.

Cellular Uptake Of The HyA-Cy5.5 Nanogels

To assess the uptake of the HyA nanogels, Caco-2 and Caco-2/HT29-MTX co-cultures were incubated for 18h with a dispersion of HyA-Cy5.5 nanogels in complete culture media. Following incubation, the cells were extensively washed, and the actin filaments stained using phalloidin-TRITC and imaged as detailed in 2.6.2.

Trans-Epithelial Electrical Resistance (TEER) Measurement

The TEER was measured to assess barrier integrity, following a protocol for static epithelial models.²⁸ The cell-culture inserts were allowed to equilibrate to RT for 10 min and the TEER was measured using a Millicell[®] ERS-2 volt-ohm-meter (Merck Millipore, Billerica, MA, USA) with STX chopstick electrodes. TEER values in $\Omega \cdot \text{cm}^2$ were calculated by subtracting the TEER of cell-free transwells[®] from the cell-cultured transwell inserts, and multiplying by the surface area of the well.

Transport Across The Intestinal Epithelium

To evaluate the capacity of the HyA-Cy5.5 nanogels to cross the intestinal epithelium, Caco-2 monocultures and co-cultures of Caco-2/HT29-MTX grown on transwell[®] inserts were distributed evenly, based on TEER, into 12-well plates pre-filled with 1.5 mL of warm HBSS. HyA-Cy5.5 nanogels in HBSS were added to the apical chamber and the cells were incubated in a humidified chamber at 37 °C for 1 h under agitation (100 rpm). At pre-determined

time-points (1, 2, 3 and 4h), 200 μL were collected from the basolateral chamber and replenished with fresh HBSS. At the 4h time-point, the samples from the apical chamber were collected and pooled for analysis. The cells were washed and incubated for 30 min in warm HBSS before measurement of the TEER to validate the integrity of the barrier. Finally, the cells were lysed with a 1% triton X-100 solution in HBSS, spun down and the supernatant collected for analysis. The HyA-Cy5.5 nanogels fluorescence was quantified by fluorescence spectroscopy ($\lambda_{\text{ex}}=650 \text{ nm}$, $\lambda_{\text{em}}=690 \text{ nm}$).

Statistical Analyses

Results are displayed as Mean \pm SD unless otherwise stated. The statistical significance was tested using the Student's *t*-test for independent samples or a two-way ANOVA with Tukey's post-hoc test using GraphPad Prism 8.2.1 (San Diego, CA, USA).

Results And Discussion

Synthesis And Characterisation Of HyA Nanogels

Amphiphilic hyaluronic acid conjugates were synthesised by grafting 16-carbon alkyl chains to the HyA backbone. The reaction was confirmed by ¹H NMR (ESI Figure 1) and the degree of substitution calculated showing a ratio of 16 alkyl chains grafted per every 100 disaccharide units (16%). C16-HyA was fluorescently labelled with Cy5.5 by the formation of stable amide bonds after reaction with Cy5.5 hydrazide in diH₂O. Figure 2A shows the fluorescence spectra of the C16-HyA-Cy5.5 before and after filtration through the 10 kDa MWCO Amicon Ultra-15

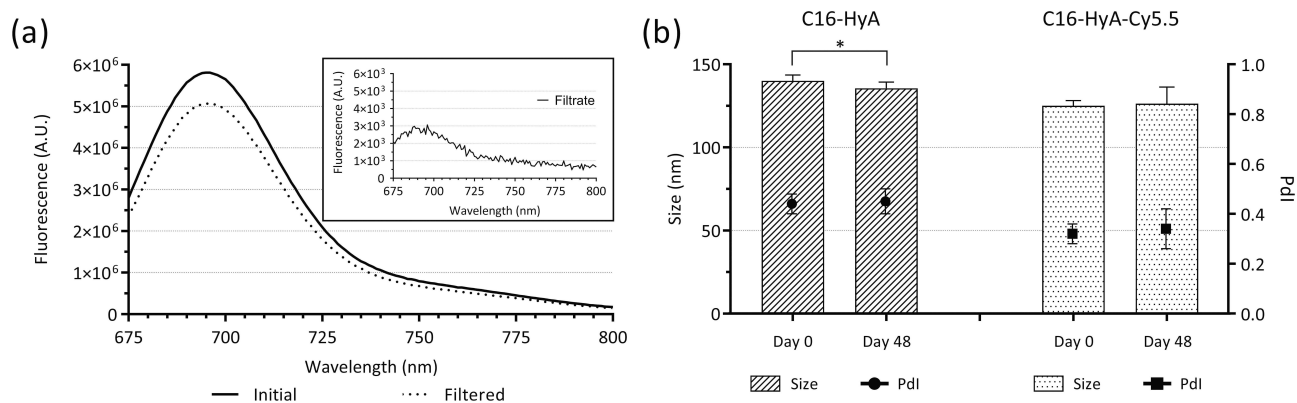


Figure 2 (A) Fluorescence emission spectra ($\lambda_{\text{ex}}=650 \text{ nm}$) of the C16-HyA-Cy5.5 conjugates before and after filtration through 10 kDa MWCO Amicon Ultra-15 centrifugal filters. The top-right rectangle shows the emission spectrum of the filtrate. **(B)** Average size and polydispersity index (Pdl) of the C16-Hya and C16-Hya-Cy5.5 nanogels measured by dynamic light scattering before and after storage for 48 days at 4 °C. Values show Mean \pm SD (N=6; **p* < 0.05 with *p*-values obtained using the Student's *t*-test for independent samples).

centrifugal filters, as well as of the filtrate. For sterility, C16-HyA-Cy5.5 was further filtered through a 0.45- μm PVDF syringe filter, which did not alter the fluorescence intensity (ESI Figure 2).

C16-HyA and C16-HyA-Cy5.5 nanogels were formed by self-assembly in water. To assess whether grafting of the Cy5.5 fluorophore affected the properties of the nanogels, both formulations were tested for their size, polydispersity index (PDI) and zeta potential by dynamic light scattering (DLS). As could be anticipated, both formulations showed high negative zeta potential (-66.4 ± 1.4 mV and -57.6 ± 6.2 mV for C16-HyA and C16-HyA-Cy5.5, respectively) due to the presence of ionisable carboxylic groups in the HyA backbone. High zeta potential values (positive or negative), are indicative of a predominance of repulsive over attractive electrostatic forces, leading to stable colloidal dispersions. In contrast, low zeta potential values are typically linked to aggregation or flocculation, though stable dispersions can also be achieved with low or neutral zeta potential.^{29–31} The decrease in the zeta potential of the C16-HyA-Cy5.5 nanogels is likely due to a reduction of free carbonyl groups, used for the formation of amide bonds after reaction with the Cy5.5 hydrazide. Though statistically significant ($p < 0.01$, Student's *t*-test), the difference of 8.8 mV, should not affect the stability of the nanogels dispersion since the surface charge remains highly negative. In addition, negatively charged particles have been linked to higher uptake and lower toxicity when compared to positively charged particles.³²

The average size of the C16-HyA and C16-HyA-Cy5.5 nanogels was 140.1 ± 3.6 nm and 125.1 ± 3.2 nm respectively. Interestingly, the modification with Cy5.5 led to a reduction in the average particle size. The achieved particle size is favourable within the context of drug delivery as nanoparticles of sizes around 100 nm have been shown to outperform other particle sizes ranging from 50 to 1,000 nm in terms of uptake by Caco-2 cells.³³

The stability of the C16-HyA and C16-HyA-Cy5.5 nanogels was evaluated by measuring the average particle size and PDI after storage for 48 days at 4 °C. A minor decrease in the particle size of C16-HyA nanogels could be observed (Figure 2B) but despite the statistical significance ($p < 0.05$, Student's *t*-test), owing to small standard deviations, this was just in the order of 3% and should be disregarded. The size of the C16-HyA-Cy5.5 remained unchanged and thus it can be concluded that both nanogel formulations remained stable for the period of 48 days.

Finally, given the nanogels were designed to be delivered orally, the stability of the nanogels was assessed at pH 5.0 and 3.0 (representative of digestion conditions) for up to 6 days (ESI Figure 3). The dispersion of the nanogels at pH 3 led to a slight increase in the average size of the nanogels to 160.9 ± 5.1 nm. Nevertheless, both size and PDI of the nanogels remained stable at both pH for up to 6 days when stored at room temperature. There was again a minor decrease in the particle size of the C16-HyA nanogels at pH 3 over time, which was statistically significant ($p < 0.05$), but should have no effect on the functionality of the nanogels. This showed that the C16-HyA nanogels remain stable at the range of pH found in the gastrointestinal tract during digestion.

Biocompatibility Of The C16-HyA Nanogels

The biocompatibility of the C16-HyA nanogels was assessed as a function of their concentration (0.01; 0.05 and 0.1 $\text{mg}\cdot\text{mL}^{-1}$) after incubation with Caco-2 cells for 24 and 48h. The cell viability was determined indirectly by assessing cell metabolic activity using the resazurin reduction assay. Figure 3 shows that the viability of the Caco-2 cells was significantly reduced ($p < 0.001$) after incubation with DMSO (positive control). In contrast, irrespective of incubation time, incubation with the C16-HyA nanogels did not produce any effect in the metabolic activity of Caco-2 cells for the range of concentrations tested. These results show that the C16-HyA nanogels are non-toxic to Caco-2 cells up to the concentration of 0.1 $\text{mg}\cdot\text{mL}^{-1}$.

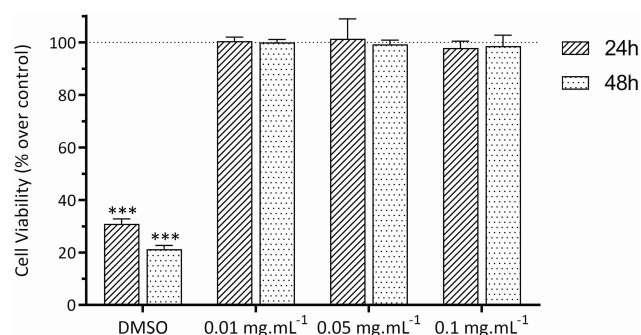


Figure 3 Effect of the C16-HyA-Cy5.5 nanogels on the viability of Caco-2 cells after incubation for 24 and 48 hrs at the concentration of 0.01, 0.05 and 0.1 $\text{mg}\cdot\text{mL}^{-1}$. The cell viability was determined indirectly by measuring fluorescence using the resazurin reduction assay ($\lambda_{\text{ex}}=560$ nm, $\lambda_{\text{em}}=590$). DMSO and PBS were used as positive and negative (100% cell viability) controls, respectively. Values show Mean \pm SD (N=8 from 2 independent assays; *** $p < 0.001$ with *p*-values obtained using the Student's *t*-test for independent samples).

Uptake And Transport Of C16-HyA-Cy5.5 Nanogels Using In Vitro Models Of The Intestinal Epithelium

Prior to the uptake and transport studies, Caco-2, HT-29 and HT29-MTX cell lines, and co-culture combinations thereof, were evaluated for their capacity to replicate a functional intestinal epithelium. Accordingly, mucus secretion, the morphology of the epithelium, tight-junction protein expression and the barrier integrity were evaluated.

Mucus Secretion

The capacity to secrete mucus is fundamental to the establishment of a physiologically relevant in vitro intestinal model. Indeed, the presence of a mucus layer is considered the first level of defence against the entry of pathogens through the gastrointestinal tract.³⁴ From a drug delivery perspective, mucus acts as an additional barrier limiting diffusion³⁵ but also potentially increasing the residence time of mucoadhesive carriers.³⁶⁻⁴⁰ This evidences the importance of addressing this fundamental parameter in the development of carriers for sustained release.

Single cultures of Caco-2, HT-29 and HT29-MTX, as well as co-cultures of Caco-2/HT-29 and Caco-2/HT29-MTX were grown for 21 days and the production of mucus assessed by staining using alcian blue. **Figure 4** shows that, as anticipated, Caco-2, HT-29 and the Caco-2/HT-29 co-culture were negative for the alcian blue staining and thus do not produce mucus. In opposition, both HT29-MTX and the co-culture of Caco-2 with HT29-MTX showed extensive mucus production. Interestingly, while the presence of mucus on the HT29-MTX cultures was

dispersed over the cell layer, on the Caco-2/HT29-MTX co-culture, the mucus was concentrated in patches (**Figure 4**, black arrows), likely related to the 9:1 seeding ratio of the two cell lines.

Morphology And Formation Of Tight Junctions

The morphology of the cell layers was assessed following 21 days of culture by staining F-actin using rhodamine-labelled phalloidin. **Figure 5** shows staggering differences between the 5 cultures conditions tested. The most significant difference was the thickness of the cell layers which rounded 10 μm for the Caco-2 and Caco-2/HT-29 co-culture but was at least twice as thick for the monocultures of both goblet cell types (more columnar), as well as for the co-culture of Caco-2/HT29-MTX. In addition, while the distribution of F-actin (green) appears to be fairly homogeneous for the monocultures of Caco-2 and HT29 and the co-culture of these, it appears more concentrated in the apical side for the HT29-MTX and the co-culture of Caco-2/HT29-MTX, suggesting that this co-culture conditions lead to the formation of a polarised epithelium, with apical microvilli forming brush borders.⁴¹ Given that HT-29 and HT29-MTX are distinguished by the capacity of the latter to produce mucus, this suggests that the presence of mucus is important to lead to cell polarisation and achieve a physiologically relevant predictive model. It was also interesting to perceive that the Caco-2/HT29-MTX co-culture recreates undulating human intestinal villi with areas of higher thickness interspersed with areas of lower thickness.⁴² This phenomenon is further verified by the images in **Figure 6**. Here, in addition to F-actin (red), the tight-junction specific protein occludin (green) was labelled to assess the

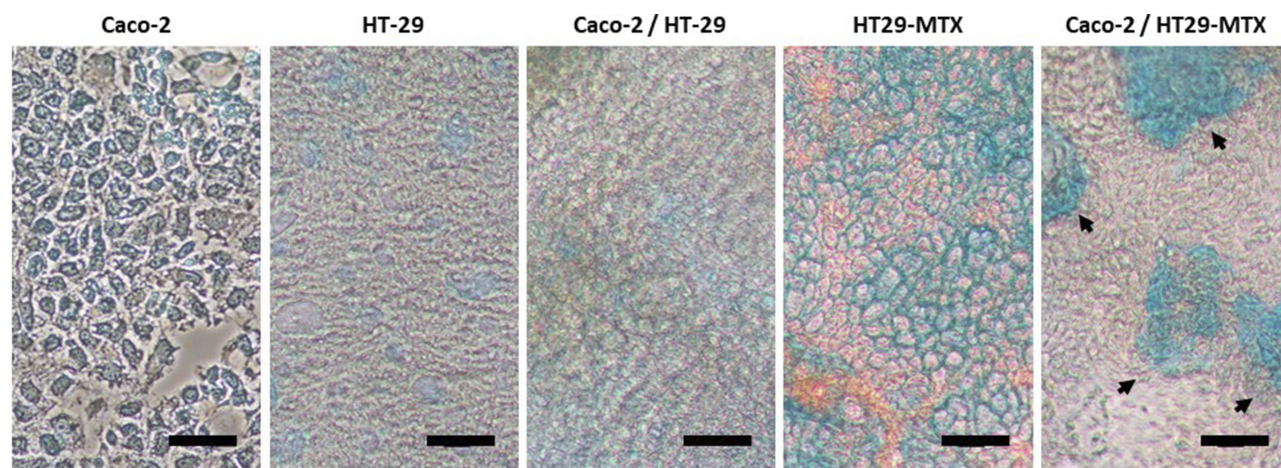


Figure 4 Optical microscopy images of single cultures of Caco-2, HT-29 and HT29-MTX, and co-cultures of Caco-2/HT-29 and Caco-2/HT29-MTX after 21 days of culture in ibidi 8-well chamber μ -slides. The cells were stained with alcian blue to show the presence of mucus (black arrows). Scale bar: 20 μm .

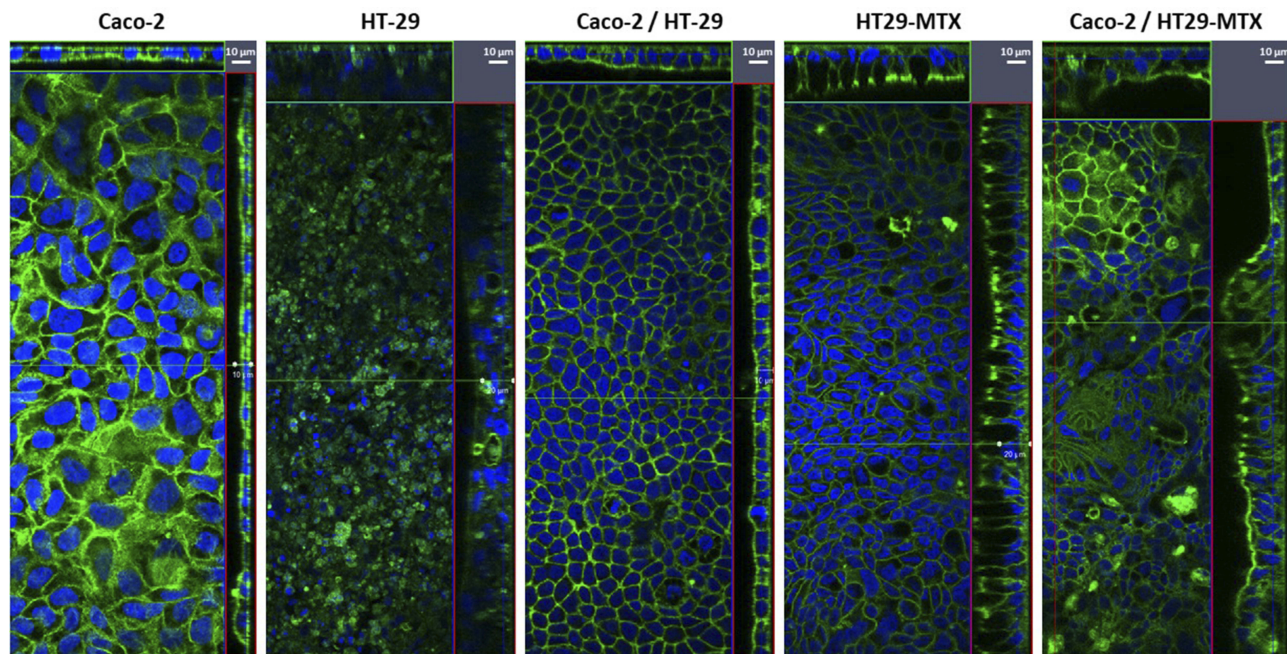


Figure 5 Laser scanning confocal microscopy images of F-actin (green) and nuclei (DAPI, blue) of Caco-2, HT-29 and HT29-MTX monocultures and co-cultures of Caco-2/HT-29 and Caco-2/HT29-MTX.

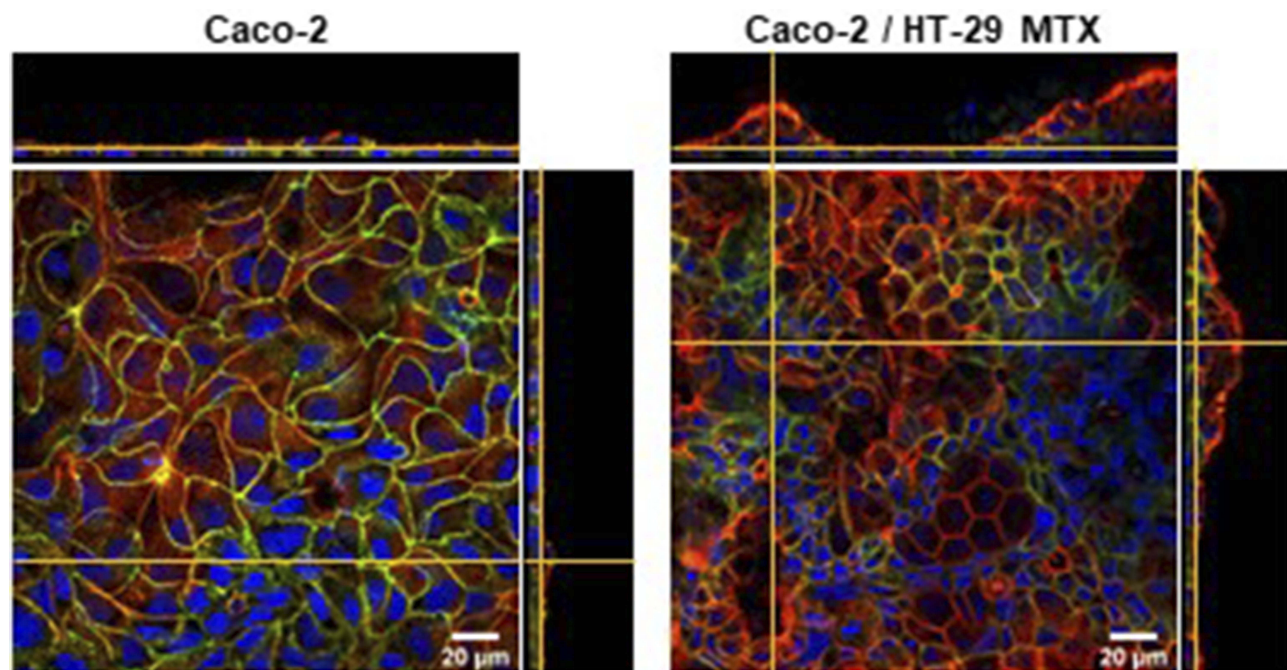


Figure 6 Laser scanning confocal microscopy images of f-actin (red), occludin (green) and nuclei (DAPI, blue) of a single culture of Caco-2 cells and Caco-2/HT-29 MTX co-culture. The images show the staggering difference in the topography of both culture conditions. The formation of a tighter barrier in the Caco-2 monolayer is evidenced by the homogeneous distribution of the tight-junction protein occludin.

formation of a tight intestinal epithelial barrier. Though not quantitative, it is apparent that the expression of occludin is more marked on the Caco-2 monoculture when compared to the Caco-2/HT29-MTX co-culture. Note that the exposure

time and power of the lasers were kept constant for the acquisition of both images. These results are in keeping with previous observations that Caco-2 monolayers show very low permeability but that the co-culture with additional

cell types has the capacity to better approximate the physiology of the in vivo scenario.²

Cellular Uptake And Intestinal Permeability

To assess the uptake of the C16-HyA-Cy5.5 nanogels, single cultures of Caco-2 and HT29-MTX, and Caco-2/HT29-MTX co-cultures were incubated with a C16-HyA-Cy5.5 nanogel solution for 18 hrs and observed by laser scanning confocal microscopy. Figure 7 shows images of a representative slice and orthogonal views of the 3 culture conditions. The orthogonal views showed that the C16-HyA-Cy5.5 nanogels were not internalised in the single cultures of HT29-MTX. This was likely due to the presence of a homogeneous mucus layer and suggests mucoadhesive properties of the HyA nanogels which remained adsorbed after several washes. In contrast, the nanogels were uptaken by both the Caco-2 monoculture and the Caco-2/HT29-MTX co-culture where they appear disperse in the cytoplasm (Figure 7, bottom). Between these two culture conditions, the uptake seemed higher for the

single culture of Caco-2 but it was difficult to discern from this study alone.

Studies of the intestinal permeability allowed to quantify the cellular uptake of the single cultures of Caco-2 and the Caco-2/HT29-MTX co-cultures. Here, cells were cultured on 1- μ m pore size Transwell[®] inserts for 21 days. At day 21, the cultures were incubated with the C16-HyA-Cy5.5 nanogels in HBSS for 4 hrs and the amount of nanogels that were uptaken and/or permeated through the intestinal barrier was quantified by fluorescence. As a control, the amount of nanogels that remained in the apical chamber after the 4-h incubation was also determined (92.3% and 89.8% for the Caco-2 and the Caco-2/HT29-MTX cultures, respectively). During the 21 days of culture, the TEER was monitored to assess the barrier integrity. From the day of the first measurement (Day 5), the TEER of the single cultures of Caco-2 was significantly higher ($p < 0.001$) than the Caco-2/HT29-MTX co-cultures (Figure 8A). This trend was maintained during the 21 days of culture, which is in line with previous studies

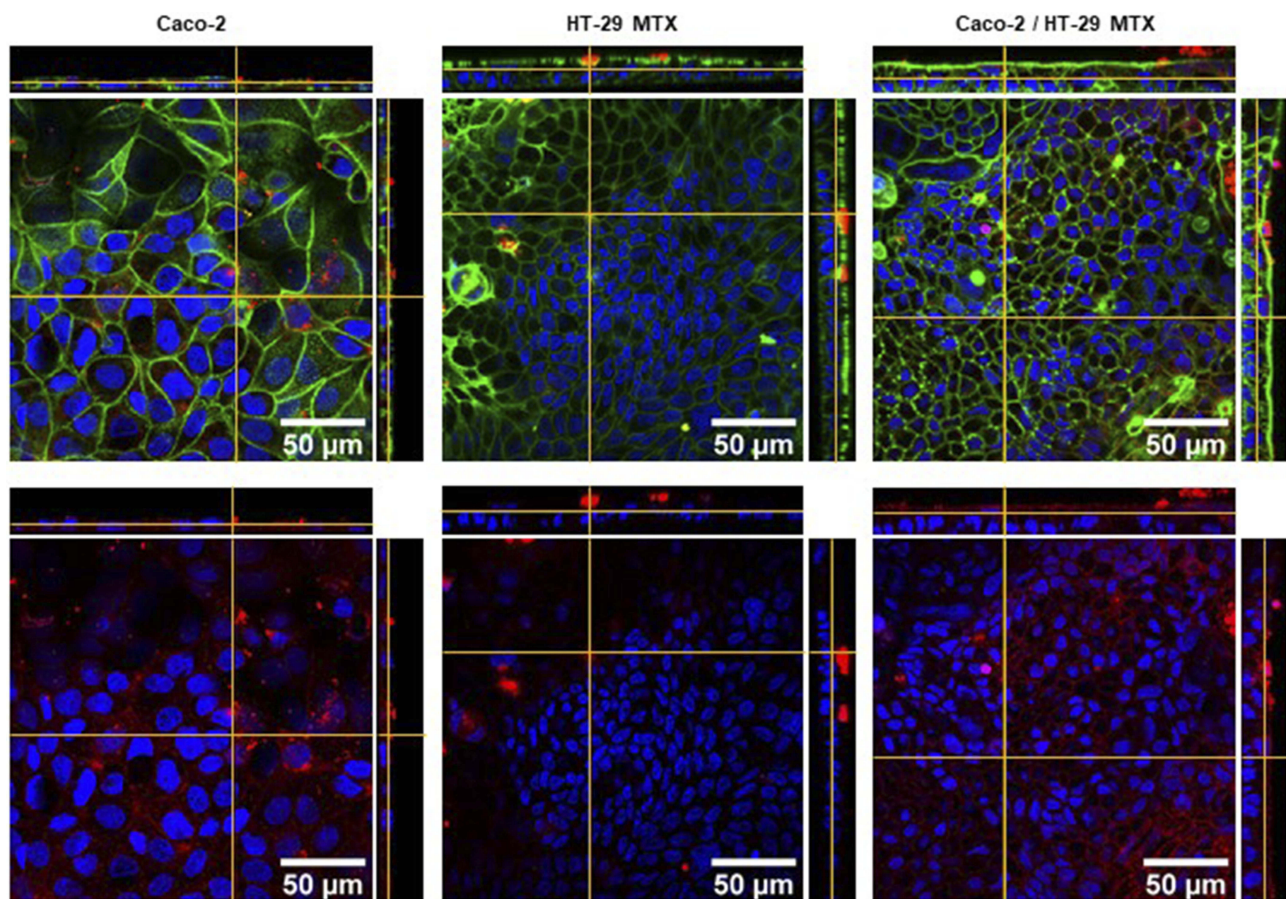


Figure 7 Laser scanning confocal microscopy images of f-actin (green), C16-HyA-Cy5.5 nanogels (red) and nuclei (DAPI, blue) of single cultures of Caco-2 and HT-29 and a Caco-2/HT-29 MTX co-culture. In the bottom images, the actin staining was omitted for clarity.

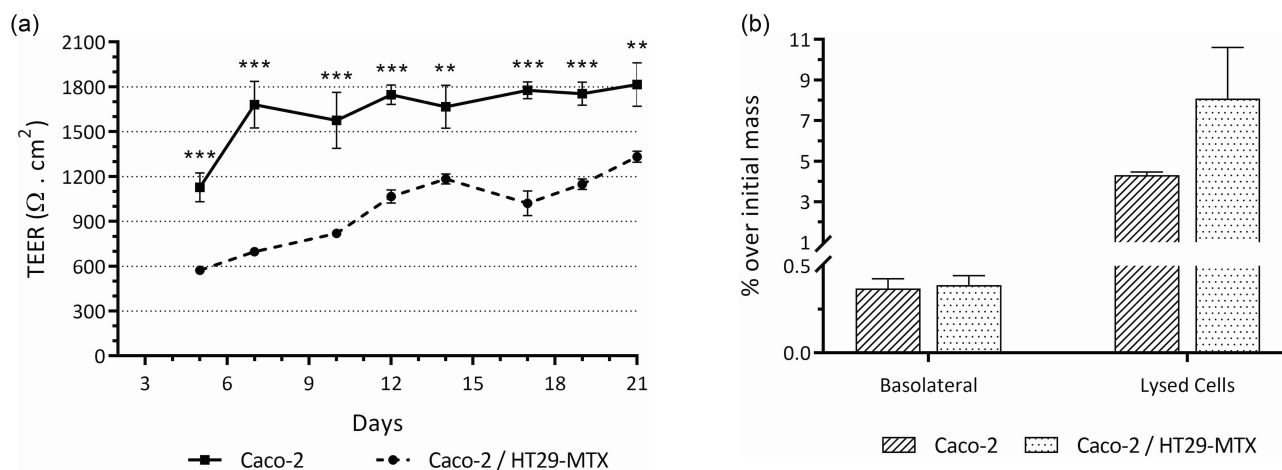


Figure 8 (A) Trans-epithelial electrical resistance (TEER) of single cultures of Caco-2 and co-cultures of Caco-2/HT29-MTX grown for 21 days on the apical chamber of 1- μ m pore size transwell® inserts. Values show Mean \pm SD (N=5; **p < 0.01; ***p < 0.001 with p-values obtained using the Student's t-test for independent samples). **(B)** Intestinal permeability of the C16-HyA-Cy5.5 nanogels incubated for 4h with the in vitro intestinal epithelial models of Caco-2 and Caco-2/HT29-MTX co-cultures grown for 21 days on the apical chamber of 1- μ m pore size transwell® inserts. Values show the mass percentage of C16-HyA-Cy5.5 nanogels found in the basolateral chamber and on lysed cells over the initial mass added to the apical chamber (Mean \pm SD; N=3).

of co-cultures of Caco-2/HT29-MTX,^{13,14,16} and supports the statement that co-cultures increase the permeability of Caco-2 approximating it to more physiological levels.^{2,12} Although not statistically significant, the amount of C16-HyA-Cy5.5 nanogels that were found either uptaken by the cells or adsorbed to the cellular layer was higher for the co-culture than for the single cultures of Caco-2 ($8.1 \pm 2.5\%$ vs $4.3 \pm 0.2\%$; Figure 8B). The amount of nanogels that effectively permeated the intestinal barrier was found to be lower than 0.5% of the initial added C16-HyA-Cy5.5 nanogel mass. Though this is a statement toward the integrity of both in vitro models, it also suggests that if the nanogels carry a bioactive that is to be administered orally and reach the systemic circulation, some degree of modification should be added to promote active transport of the nanogels.

Conclusion

This work showed the synthesis of amphiphilic hyaluronic acid by grafting of 16-carbon alkyl chains (C16). The C16-hyaluronic acid was further labelled fluorescently with a Cy5.5 dye for tracking of the cellular uptake and intestinal permeability, with no significant effect on the size and surface charge of the nanogels, which remained stable for up to 48 days. In addition, the achieved particle size of 125.1 ± 3.2 nm is favourable within the context of drug delivery as nanoparticles of sizes around 100 nm have been shown to outperform other particle sizes ranging from 50 to 1,000 nm in terms of uptake by Caco-2 cells.

Studies of biocompatibility using the resazurin reduction assay showed that the nanogels were non-toxic to the Caco-2

cell line up to the concentration of $0.1 \text{ mg} \cdot \text{mL}^{-1}$. The uptake and permeability of the nanogels were studied using in vitro intestinal models with verified production of mucus, expression of the tight-junction protein occludin and barrier integrity – monitored by the TEER. To evaluate the physiological relevance of the in vitro model, different single and co-culture conditions were studied using Caco-2, HT-29 and HT29-MTX cells. The presence of the mucus-producing HT29-MTX cells led to a thicker cell layer with columnar and polarized cells with actin concentrated in the apical side recreating the in vivo scenario. The uptake studies highlighted the importance of mucus in in vitro models mimicking the intestinal epithelium. 4.3% and 8.1% of the total mass of the added nanogels were uptaken by Caco-2 and the Caco-2/HT29-MTX co-culture respectively after 4 hrs, and less than 0.5% actually permeated the barrier to the basolateral side. The HyA nanogels were effectively uptaken and appear to be mucoadhesive remaining on the cell layer after several washes. If systemic delivery is envisaged, further modification with targeting moieties should be considered to improve the nanogel permeability. Regarding the in vitro models, based on these data, a microfluidic dynamic model is currently under development including simulated-peristaltic motion to understand the effect of continuous flow and mechanic stimulation on cell differentiation.

Acknowledgements

The authors would like to acknowledge Doctor Andreia Gomes from the University of Minho for providing the HT-29 cells. This work was funded by MICRODIGEST

project (grant agreement 037716) co-funded by FCT and ERDF through COMPETE2020, the FODIAC project (grand agreement 778299) funded by the European Commission through H2020-MSCA-RISE-2017 and CVMar+I project (INTERREG V-A España – Portugal – POCTEP 2014–2020, Ref. 0302_CVMAR_I_1_P).

Disclosure

Isabel Amado received funding from the People Programme (Marie Curie Actions) of the European Union's Seventh Framework Programme (FP7/2007-2013) under REA grant agreement no. 600391. The authors report no other conflicts of interest in this work.

References

- Sarmiento B, Andrade F, Da Silva SB, Rodrigues F, Das Neves J, Ferreira D. Cell-based in vitro models for predicting drug permeability. *Expert Opin Drug Metab Toxicol.* 2012;8:607–621. doi:10.1517/17425255.2012.673586
- Antunes F, Andrade F, Ferreira D, Mørck Nielsen H, Sarmiento B. Models to predict intestinal absorption of therapeutic peptides and proteins. *Curr Drug Metab.* 2012;14:4–20. doi:10.2174/1389200211309010004
- Li AP. Screening for human ADME/Tox drug properties in drug discovery. *Drug Discov Today.* 2001;6:357–366. doi:10.1016/S1359-6446(01)01712-3
- Hidalgo IJ, Raub TJ, Borchardt RT. Characterization of the human colon carcinoma cell line (Caco-2) as a model system for intestinal epithelial permeability. *Gastroenterology.* 1989;96:736–749. doi:10.1016/S0016-5085(89)80072-1
- YU Q, YANG Q. Diversity of tight junctions (TJs) between gastrointestinal epithelial cells and their function in maintaining the mucosal barrier. *Cell Biol Int.* 2009;33:78–82. doi:10.1016/j.cellbi.2008.09.007
- Kong S, Zhang YH, Zhang W. Regulation of intestinal epithelial cells properties and functions by amino acids. *Biomed Res Int.* 2018;2018:1–10.
- Lea T. Caco-2 cell line. In: Verhoeckx K, editor. *The Impact of Food Bioactives on Health.* Springer International Publishing; 2015:103–111. doi:10.1007/978-3-319-16104-4_10
- Shah P, Jogani V, Bagchi T, Misra A. Role of Caco-2 cell monolayers in prediction of intestinal drug absorption. *Biotechnol Prog.* 2006;22:186–198.
- Engle MJ, Goetz GS, Alpers DH. Caco-2 cells express a combination of colonocyte and enterocyte phenotypes. *J Cell Physiol.* 1998;174:362–369. doi:10.1002/(ISSN)1097-4652
- Walter E, Kissel T. Heterogeneity in the human intestinal cell line Caco-2 leads to differences in transepithelial transport. *Eur J Pharm Sci.* 1995;3:215–230. doi:10.1016/0928-0987(95)00010-B
- Artursson P, Palm K, Luthman K. Caco-2 monolayers in experimental and theoretical predictions of drug transport. *Adv Drug Deliv Rev.* 2001;46:27–43. doi:10.1016/S0169-409X(00)00128-9
- Lozoya-Agullo I, Aratijo F, González-Álvarez I, et al. Usefulness of Caco-2/HT29-MTX and Caco-2/HT29-MTX/Raji B coculture models to predict intestinal and colonic permeability compared to Caco-2 monoculture. *Mol Pharm.* 2017;14:1264–1270. doi:10.1021/acs.molpharmaceut.6b01165
- Hilgendorf C, Spahn-Langguth H, Regårdh CG, Lipka E, Amidon GL, Langguth P. Caco-2 versus Caco-2/HT29-MTX co-cultured cell lines: permeabilities via diffusion, inside- and outside-directed carrier-mediated transport. *J Pharm Sci.* 2000;89:63–75. doi:10.1002/(SICI)1520-6017(200001)89:1<63::AID-JPS7>3.0.CO;2-6
- Béduneau A, Tempesta C, Fimbel S, et al. A tunable Caco-2/HT29-MTX co-culture model mimicking variable permeabilities of the human intestine obtained by an original seeding procedure. *Eur J Pharm Biopharm.* 2014;87:290–298. doi:10.1016/j.ejpb.2014.03.017
- Mahler GJ, Shuler ML, Glahn RP. Characterization of Caco-2 and HT29-MTX cocultures in an in vitro digestion/cell culture model used to predict iron bioavailability. *J Nutr Biochem.* 2009;20:494–502. doi:10.1016/j.jnutbio.2008.05.006
- Walter E, Janich S, Roessler BJ, Hilfinger JM, Amidon GL. HT29-MTX/Caco-2 cocultures as an in vitro model for the intestinal epithelium: in vitro–in vivo correlation with permeability data from rats and humans. *J Pharm Sci.* 1996;85:1070–1076. doi:10.1021/js960110x
- Pedrosa SS, Gonçalves C, David L, Gama M. A novel crosslinked hyaluronic acid nanogel for drug delivery. *Macromol Biosci.* 2014;14:1556–1568. doi:10.1002/mabi.v14.11
- Manju S, Sreenivasan K. Conjugation of curcumin onto hyaluronic acid enhances its aqueous solubility and stability. *J Colloid Interface Sci.* 2011;359:318–325. doi:10.1016/j.jcis.2011.03.071
- Huang G, Huang H. Application of hyaluronic acid as carriers in drug delivery. *Drug Deliv.* 2018;25:766. doi:10.1080/10717544.2018.1450910
- Chen WYJ, Abatangelo G. Functions of hyaluronan in wound repair. *Wound Repair Regen.* 1999;7:79–89. doi:10.1046/j.1524-475X.1999.00079.x
- Turley EA. Hyaluronan-binding proteins and receptors. *Adv Drug Deliv Rev.* 1991;7:257–264. doi:10.1016/0169-409X(91)90005-W
- Aruffo A, Stamenkovic I, Melnick M, Underhill CB, Seed B. CD44 is the principal cell surface receptor for hyaluronate. *Cell.* 1990;61:1303–1313. doi:10.1016/0092-8674(90)90694-A
- Wei X, Senanayake TH, Warren G, Vinogradov SV. Hyaluronic acid-based nanogel–drug conjugates with enhanced anticancer activity designed for the targeting of CD44-positive and drug-resistant tumors. *Bioconjug Chem.* 2013;24:658–668. doi:10.1021/bc300632w
- Snipstad S, Hak S, Baghirov H, et al. Labeling nanoparticles: dye leakage and altered cellular uptake. *Cytom Part A.* 2017;91:760–766. doi:10.1002/cyto.a.22853
- Swift JL, Cramb DT. Nanoparticles as fluorescence labels: is size all that matters? *Biophys J.* 2008;95:865–876. doi:10.1529/biophysj.107.127688
- Kim YS, Ho SB. Intestinal goblet cells and mucins in health and disease: recent insights and progress. *Curr Gastroenterol Rep.* 2010;12:319–330. doi:10.1007/s11894-010-0131-2
- Gagnon M, Zihler Berner A, Chervet N, Chassard C, Lacroix C. Comparison of the Caco-2, HT-29 and the mucus-secreting HT29-MTX intestinal cell models to investigate Salmonella adhesion and invasion. *J Microbiol Methods.* 2013;94:274–279. doi:10.1016/j.mimet.2013.06.027
- Gaillard PJ, De Boer AG. Relationship between permeability status of the blood-brain barrier and in vitro permeability coefficient of a drug. *Eur J Pharm Sci.* 2000;12:95–102. doi:10.1016/S0928-0987(00)00152-4
- Hanaor D, Michelazzi M, Leonelli C, Sorrell CC. The effects of carboxylic acids on the aqueous dispersion and electrophoretic deposition of ZrO₂. *J Eur Ceram Soc.* 2012;32:235–244. doi:10.1016/j.jeurceramsoc.2011.08.015
- Hotze EM, Phenrat T, Lowry GV. Nanoparticle aggregation: challenges to understanding transport and reactivity in the environment. *J Environ Qual.* 2010;39:1909. doi:10.2134/jeq2009.0462
- Schäfer B, Hecht M, Harting J, Nirschl H. Agglomeration and filtration of colloidal suspensions with DVLO interactions in simulation and experiment. *J Colloid Interface Sci.* 2010;349:186–195. doi:10.1016/j.jcis.2010.05.025
- Bannunah AM, Vllasaliu D, Lord J, Stolnik S. Mechanisms of nanoparticle internalization and transport across an intestinal epithelial cell model: effect of size and surface charge. *Mol Pharm.* 2014. doi:10.1021/mp500439c
- Yin Win K, Feng -S-S. Effects of particle size and surface coating on cellular uptake of polymeric nanoparticles for oral delivery of anticancer drugs. *Biomaterials.* 2005;26:2713–2722. doi:10.1016/j.biomaterials.2004.07.050

34. Hansson GC. Role of mucus layers in gut infection and inflammation. *Curr Opin Microbiol.* 2012. doi:10.1016/j.mib.2011.11.002
35. Boegh M, Nielsen HM. Mucus as a barrier to drug delivery - understanding and mimicking the barrier properties. *Basic Clin Pharmacol Toxicol.* 2015;116:179–186. doi:10.1111/bcpt.2015.116.issue-3
36. Hodayun B, Lin X, Choi H-J, Hodayun B, Lin X, Choi H-J. Challenges and recent progress in oral drug delivery systems for biopharmaceuticals. *Pharmaceutics.* 2019;11:129. doi:10.3390/pharmaceutics11030129
37. Boddupalli BM, Mohammed ZNK, Nath RA, Banji D. Mucoadhesive drug delivery system: an overview. *J Adv Pharm Technol Res.* 2010;1:381–387. doi:10.4103/0110-5558.76436
38. Netsomboon K, Bernkop-Schnürch A. Mucoadhesive vs. mucopentrating particulate drug delivery. *Eur J Pharm Biopharm.* 2016;98:76–89. doi:10.1016/j.ejpb.2015.11.003
39. Arora S, Bisen G, Budhiraja R. Mucoadhesive and muco-penetrating delivery systems for eradication of helicobacter pylori. *Asian J Pharm.* 2012;6:18. doi:10.4103/0973-8398.100127
40. Ensign LM, Cone R, Hanes J. Oral drug delivery with polymeric nanoparticles: the gastrointestinal mucus barriers. *Adv Drug Deliv Rev.* 2012;64:557–570. doi:10.1016/j.addr.2011.12.009
41. Ubelmann F, Chamailard M, El-Marjou F, et al. Enterocyte loss of polarity and gut wound healing rely upon the F-actin-severing function of villin. *Proc Natl Acad Sci.* 2013;110:E1380–E1389. doi:10.1073/pnas.1218446110
42. Kim HJ, Ingber DE. Gut-on-a-Chip microenvironment induces human intestinal cells to undergo villus differentiation. *Integr Biol.* 2013;5:1130. doi:10.1039/c3ib40126j

International Journal of Nanomedicine

Dovepress

Publish your work in this journal

The International Journal of Nanomedicine is an international, peer-reviewed journal focusing on the application of nanotechnology in diagnostics, therapeutics, and drug delivery systems throughout the biomedical field. This journal is indexed on PubMed Central, MedLine, CAS, SciSearch®, Current Contents®/Clinical Medicine,

Journal Citation Reports/Science Edition, EMBase, Scopus and the Elsevier Bibliographic databases. The manuscript management system is completely online and includes a very quick and fair peer-review system, which is all easy to use. Visit <http://www.dovepress.com/testimonials.php> to read real quotes from published authors.

Submit your manuscript here: <https://www.dovepress.com/international-journal-of-nanomedicine-journal>